J Mater Sci (2010) 45:124–129
DOI 10.1007/s10853-009-3901-1

# Direct detection of electron spins and doping effects in spin-polarized electron transport in gallium arsenide

**M. Idrish Miah**

Received: 24 March 2009 / Accepted: 15 September 2009 / Published online: 8 October 2009
© Springer Science+Business Media, LLC 2009

**Abstract** The spin Hall effect allows the direct detection of spins in semiconductors. In this study, electron spins in *n*-doped gallium arsenide are detected and the effects of *n*-type doping in gallium arsenide under drift are studied. It is found that the effects in the spin-polarized electron transport increase with increasing doping density in the moderate range, indicating that the introduction of *n*-type dopants increases the electron-spin lifetimes in gallium arsenide. However, the transport drifting by a high field shows no effects because of destroying the electron-spin polarization in *n*-doped gallium arsenide. The results are discussed in details.

## Introduction

As an electron bears spin as well as charge, combining carrier spin as a new degree of freedom with the established charge-based microelectronic engineering of modern devices offers exciting opportunities for new functionality and performance. This approach is referred to as "semiconductor spintronics" [1, 2]. However, the functionality and performance of semiconductor spintronic devices require the efficient injection (such that the spins can be transported reliably over reasonable distances) and the detection of electron spins in semiconductors. Much effort has thus been made towards understanding the injection and detection of spins in semiconductors [1, 3, 4].

The injection of spins into a semiconductor has been achieved either by optical excitations [3], or mostly by magnetic materials or ferromagnetic contacts [5–7]. Several attempts, e.g., using ferromagnetic contacts to Si or InAs-based quantum wells (two-dimensional electron gas structures), have resulted in modest spin-injection effects measured at 1% or even below [6, 7]. Such small effects make it difficult to either unambiguously confirm spin injection or successfully implement new device concepts. The "conductivity mismatch," or more precisely, a mismatch between effective resistances in the metal and in semiconductor host, appears to be the limiting factor [7].

For optical excitation of bulk zinc-blende semiconductors, such as gallium arsenide, with photon energy just above the bandgap $E_g$ (but low enough to avoid exciting carriers from the split-off band), because of the selection rules (Fig. 1, left) governing optical transitions from heavy-hole or light-hole states to conduction-band states, right circular polarization ($\sigma^+$) generates a density of spin-down electrons ($n_\downarrow$), which is three times the density of spin-up electrons ($n_\uparrow$), and vice versa for left circularly polarized light ($\sigma^-$) [8]. Hence, the initial electron-spin polarization ($p_0$) generated by a $\sigma^\pm$ beam in a zinc-blende semiconductor, defined as $p(\vec{r},t) = \left(n_\downarrow(\vec{r},t) - n_\uparrow(\vec{r},t)\right)/\left(n_\downarrow(\vec{r},t) + n_\uparrow(\vec{r},t)\right)$, is ±0.5 (50%). Optical excitation with $\sigma^+$ ($\sigma^-$) injects spins along the direction parallel (antiparallel) to the direction of the light propagation, i.e., $\sigma^+$ ($\sigma^-$) injects spins along –*z*(*z*) (Fig. 1, right). As optically induced hole-spin relaxation is extremely fast (≤100 fs), their polarization is effectively zero and need not be considered [3].

M. Idrish Miah (✉)
Queensland Micro- and Nanotechnology Centre, Griffith University, Nathan, Brisbane, QLD 4111, Australia
e-mail: m.miah@griffith.edu.au

M. Idrish Miah
School of Biomolecular and Physical Sciences, Griffith University, Nathan, Brisbane, QLD 4111, Australia

M. Idrish Miah
Department of Physics, University of Chittagong, Chittagong, Chittagong 4331, Bangladesh

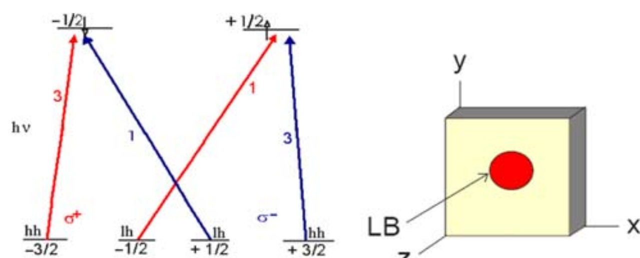


**Fig. 1** The selection rules for the transitions from the heavy-hole (*hh*), light-hole (*lh*) valence bands to conduction band. The allowed transitions for $\sigma^+$ ($\Delta m_j = +1$) and $\sigma^-$ ($\Delta m_j = -1$) are shown by the *red* and *green lines* respectively, where $\sigma^+$ for right and $\sigma^-$ for left circularly polarized light. The *numbers near the lines* represent the relative-transition probabilities. The degenerate states (energy levels) at $\boldsymbol{k} = 0$ are labeled by their $m_j$ quantum numbers. The small ↑ and ↓ in conduction band indicate the electron's spin orientations. On the *right*, a schema showing the directions of the light-beam (LB) propagation and the spin injection. The $\sigma^+$ and $\sigma^-$ light inject spins along the directions –*z* and *z*, respectively. (Color figure online)

While the detection of spins in semiconductors has previously been obtained mainly through optical methods [3], a direct or electrical means of detecting spins is very desirable for fully exploring the possibility of utilizing the spin degree of freedom and spintronic-device applications. The spin Hall effect (SHE) has recently been proposed (also observed [9] using Kerr rotation microscopy to detect spin current optically) to be a convenient and useful tool for directly detecting spins or spin currents in paramagnetic metals or semiconductors [10]. The SHE thus provides new manipulation techniques for converting electrical currents into spin currents.

Here, we directly detect bias-dependent electron spins by the optically spin-induced Hall effect [11] in the absence of the external magnetic field in devices of moderately *n*-doped gallium arsenide. The nonequilibrium magnetization for the effect is induced optically by injecting spin-polarized electrons into the device. The effects of *n*-type doping in gallium arsenide under drift are studied. The results are presented by discussing the dominant spin-relaxation mechanism in *n*-doped gallium arsenide at room temperature.

## Device fabrication and measurements

### Sample preparation

Devices were fabricated on doped gallium arsenide with various doping densities: $n = 5 \times 10^{21}$, $1 \times 10^{22}$, $3 \times 10^{22}$, and $1 \times 10^{23}$ $m^{-3}$. The *n*-type doping (Si) was used to achieve long spin lifetimes $\tau_s$ [3]. Au/Ge/Pd contacts were deposited lithographically, with Pd layers adjacent to the gallium arsenide substrates, using an e-beam evaporator with a base pressure of $\sim 5 \times 10^{-8}$ Torr. The contact metallization was annealed in a tube furnace in flowing nitrogen at temperature of 180 °C for 1 h to achieve reliable (ohmic) contacts. A gold wire was bonded to the center of each of four contacts and the sample chip was mounted in a chip carrier.

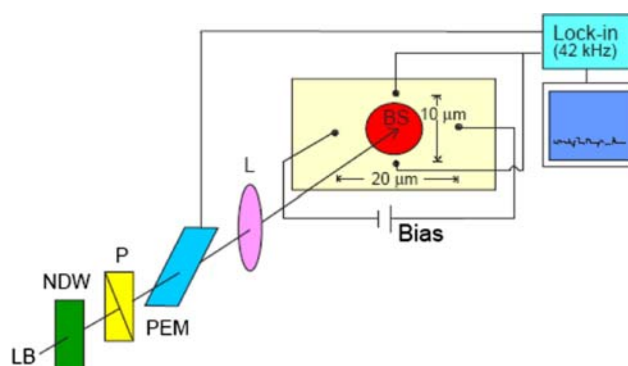


**Fig. 2** A schema of the experimental set-up for the optically induced spin detection and for the study of spin-polarized electron transport under external electric field. *LB* Laser beam, *NDW* neutral density wheel, *P* polarizer, *PEM* photo-elastic modulator, *L* lens, *BS* beam spot

### Experimental details

Figure 2 shows a schema of the spin-detection experimental setup, along with the geometry of the sample. For optical excitation, a mode-locked Ti:sapphire laser, which generated ps pulses at a 76 MHz repetition rate was used. The excitation photon energy was tuned slightly above the bandgap of gallium arsenide ($\lambda \sim 800$ nm). A neutral density wheel was used to vary the optical power. The average power on the sample was 4 mW. The polarization of the beam was modulated using a photo-elastic modulator at a lock-in reference frequency of 42 kHz. The laser beam was focused to a $\sim$6 µm (full wave at half maximum) spot at the surface of the sample. Care was taken not to illuminate any of the electrical contacts to avoid the generation of any artifacts. The spot size was measured by knife-edge scans and the spatial profile of the pulse was found to be Gaussian. The modulated spin-induced Hall voltage was measured by a lock-in amplifier at room temperature.

## Results and discussion

Electrons in the samples were spin-oriented by pumping them with a $\sigma^{\pm}$ beam. The spin–orbit coupling in a nonmagnetic semiconductor produces left–right asymmetric scattering of the electrons for a fixed spin orientation. The spin-up electrons, for example, tend to be scattered to the right more than to the left via skew-scattering and side jump. If the longitudinal current is spin-polarized, e.g.,

current carriers contain more spin-up electrons than spin-down electrons, there would be more electrons scattered to the right than to the left. This leads to both spin and charge accumulations in the transverse direction of the sample [12, 13]. When the spin-polarized electrons are dragged by an external electric field in the device, as depicted in Fig. 2, a spin-induced Hall voltage ($V_{sH}$) as a measure of the net charge accumulation is observed.

Our experiment, therefore, investigates the effect of a longitudinal electric field on the spin-oriented electrons induced by a circularly polarized light and detects electron spins by observing the effect (the transverse Hall field, $E_{sH}$) resulting from spin-polarized electrons accumulating at the transverse edges of the sample as a result of left–right asymmetries in scattering for spin-up and spin-down electrons in the presence of spin–orbit interaction.

The results obtained from the spin-detection experiments are presented in Figs. 3, 4, 5, 6, 7, 8, and 9. Figure 3 shows typical scans for a sample at two different field strengths. In Figs. 4, 5, 6, and 7, we plot the weak-to-moderate electric field and moderate doping density dependences of $V_{sH}$, where an average of the data taken from several experiments was calculated. As can be seen from Figs. 4 and 5, $V_{sH}$ increases quickly to a maximum value and remains almost constant. In the weak field, the dependence of $V_{sH}$ was found to be linear (Fig. 5), like the ordinary Hall effect. Figure 6 shows the ranges of constancy of the signals for all the samples. As seen, $V_{sH}$ and thus polarization (or $\tau_s$ of the photo-injected electrons) is preserved during transport in $n$-type gallium arsenide in moderate electric fields, which is very important for implementing spin-sensitive new device ideas. Although the spin for a moderate electric field is preserved, the spin-relaxation rate becomes considerably larger for higher fields, as will be shown later.

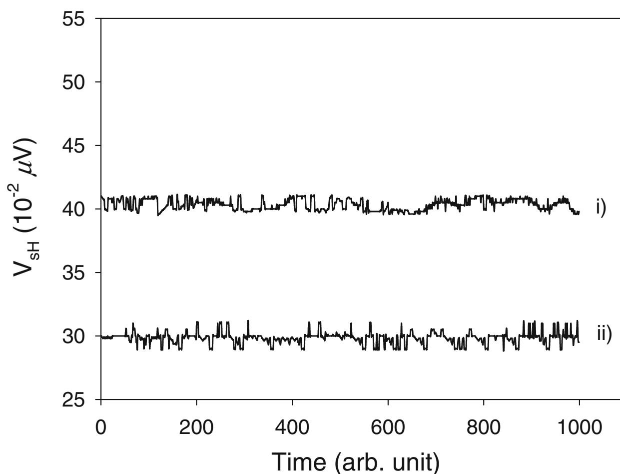


**Fig. 3** Signals: typical scans for a sample ($1 \times 10^{17}$ cm$^{-3}$) at fields (i) 95 and (ii) 5 mV μm$^{-1}$

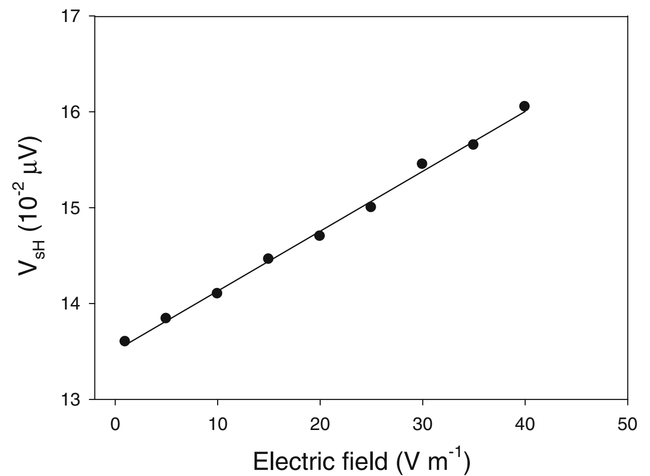


**Fig. 4** Weak field dependence of the Hall voltage for a sample ($1 \times 10^{17}$ cm$^{-3}$). *Solid line* is a linear fit to the experimental data

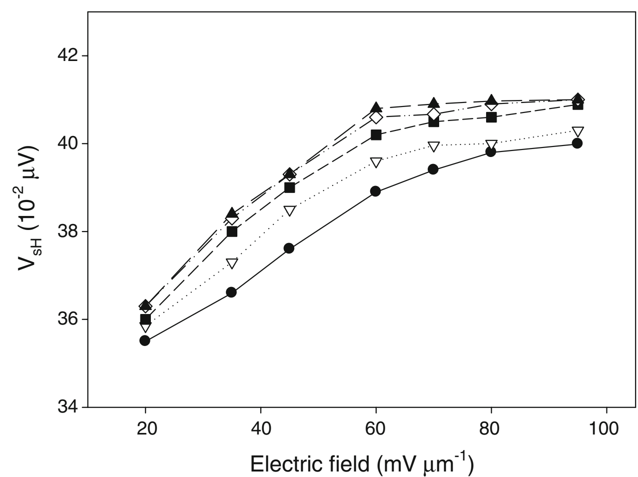


**Fig. 5** Moderate field dependence of $V_{sH}$ (*circle*: $5 \times 10^{15}$ cm$^{-3}$; *triangle down*: $1 \times 10^{16}$ cm$^{-3}$; *square*: $3 \times 10^{16}$ cm$^{-3}$; *diamond*: $1 \times 10^{17}$ cm$^{-3}$; *triangle up*: $2 \times 10^{17}$ cm$^{-3}$)

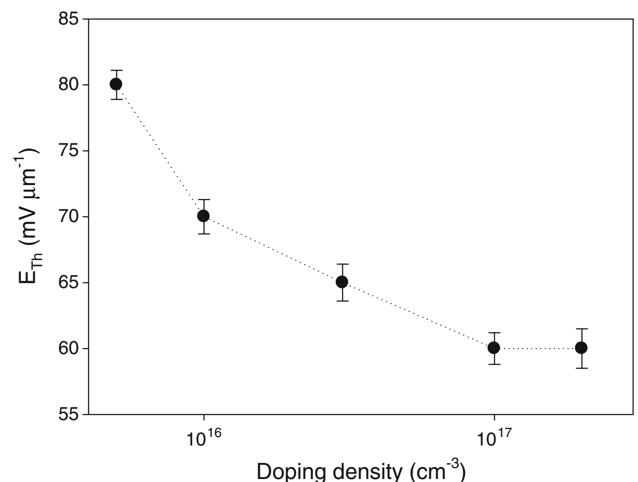


**Fig. 6** Doping-density dependence of $E_{Th}$

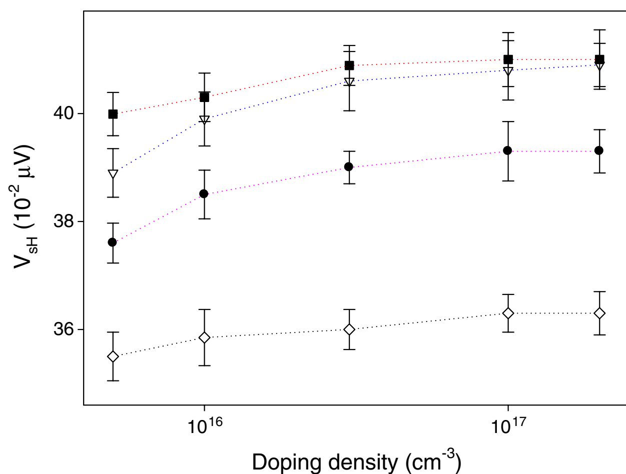


**Fig. 7** Doping-density dependence of the Hall voltage (*circle*: 45 mV μm$^{-1}$; *triangle*: 60 mV μm$^{-1}$; *square*: 95 mV μm$^{-1}$; *diamond*: 20 mV μm$^{-1}$)

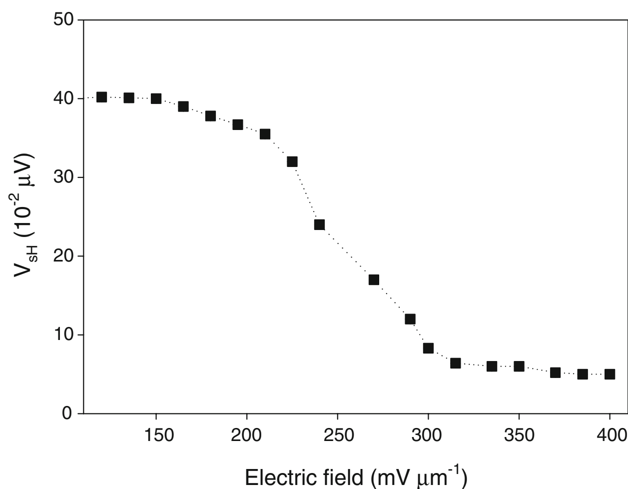


**Fig. 8** $V_{sH}$ as a function of the electric field in the high-field regime for a sample ($1 \times 10^{17}$ cm$^{-3}$)

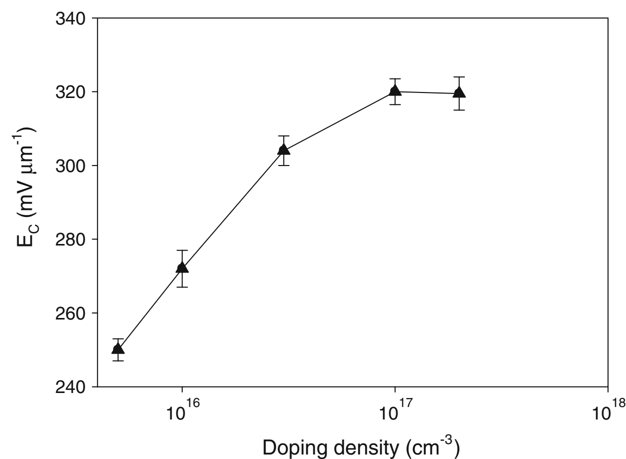


**Fig. 9** Doping density dependence of $E_C$. As can be seen, $E_C$ increases with increasing doping density within the moderate range

The lower field for which $V_{sH}$ reaches its maximum value, i.e., the threshold field $E_{Th}$, was calculated. Figure 6 shows the doping density dependence of $E_{Th}$. As seen for the two higher-doped samples, $V_{sH}$ reach maxima at 60 mV μm$^{-1}$ and remain almost constant up to $\sim$120 mV μm$^{-1}$. For the lowest-doped sample, $V_{sH}$ reaches the maximum at $\sim$80 mV μm$^{-1}$, but still remains almost constant up to about 120 mV μm$^{-1}$. The maximum value of $V_{sH} = 0.407$ μV was observed for the highest-doped sample and the minimum for the lowest-doped sample.

It is also seen from Fig. 7 that $V_{sH}$ increased with increasing doping density. The introduction of *n*-type dopants in semiconductors increases $\tau_s$, because the electronic spin polarization in these systems survives for longer times. Studies of spin precession in *n*-doped gallium arsenide reveal that moderately *n*-type doping yields significantly extended $\tau_s$ [3]. A similar trend was observed in another experiment [14], which studied the electric field dependence spin polarization of electrons in gallium arsenide and showed that several percentage of polarization increased by increasing doping by a factor of 100.

For the less-doped sample, the Hall conductivity ($\sigma_{sH}$) is low because of the higher compensation ratio [15] and the side-jump contribution dominates the effect. Although the side-jump contribution is independent of $\tau_s$, the skew-scattering contribution will grow [16] with $\tau_s$, resulting in a higher contribution to the $\sigma_{sH}$ for higher doping density, but would be cut-off when $\tau_s$ becomes comparable to the inverse of the spin–orbit splitting ($\Delta$) of the valance band at the Fermi level due to the $k^3$-Dresselhaus term [17]. For the higher-doped samples, skew scattering increases, agreeing well with the theoretical predictions performed by Tse and Sarma [18]. They considered the skew-scattering and side-jump contributions separately and calculated the $\sigma_{sH}$. Their estimation gives a value for $\sigma_{sH}$ by summing a negative side jump and a much larger positive skew-scattering contribution. Increasing doping should increase skew-scattering and decrease side jump, giving a higher positive shift to $\sigma_{sH}$ and, hence, a higher effect. The doping density dependence, as demonstrated, also agrees with the experimental results reported in reference [16].

The high-field dependence of $V_{sH}$ showing the exponential decay of the signal for a sample ($10^{17}$ cm$^{-3}$) is given in Fig. 8. Above 120 mV μm$^{-1}$, $V_{sH}$ for all samples was found to decay. It disappeared very quickly after 200 mV μm$^{-1}$. The decay of $V_{sH}$ with the field might be due to the enhanced electron-spin relaxation at higher electric fields or current densities. Although the spin for a moderate electric field was preserved (Fig. 5), a significant reduction in the spin relaxation was observed when the electrons were injected with a high field. The increasing field leads to a larger charge and spin accumulations near sample edges, but polarization saturates because of shorter

$\tau_s$ for the larger field. The suppression of $\tau_s$ with the increasing field from saturation implies that spin decay increases with field, which is consistent with other observations [19]. The drift field at which spin relaxation or depolarization occurs was found to be relatively small.

As seen, the photo-generated spin can travel without losing the initial orientation as long as their field is below a threshold value of $\sim 120$ mV $\mu m^{-1}$. Above the threshold, spin depolarization is considerably enhanced due to the enhanced spin relaxation as a result of the increase of the electron temperature. While for the highest-doped sample the electron spin disappears or is completely lost for fields higher than 320 mV $\mu m^{-1}$, the electron spin for lowest-doped sample is found to disappear for fields $\geq$250 mV $\mu m^{-1}$. Our results agree with those of the field-dependent spin transport experiments by Sanada et al. [19]. These authors studied spin relaxation of photo-generated electrons during drift transport in gallium arsenide at low temperatures by photoluminescence measurements. They showed that the photo-injected spins could travel without losing their initial spin orientation as long as the field was below 100 mV $\mu m^{-1}$ and the spin relaxation rate increased rapidly with the field, and polarization disappeared at $\sim$350 mV $\mu m^{-1}$. It is noted that the photo-injected spins in their study were generated with a much higher optical power.

The origin of field-dependent efficient electron-spin relaxation in *n*-doped gallium arsenide is discussed based on the D'yakonov–Perel' (DP) spin relaxation mechanism [13]. The DP mechanism is due to spin–orbit coupling in semiconductors lacking inversion symmetry. In III–V semiconductors, such as gallium arsenide, the degeneracy in the conduction band is lifted for $\vec{k} \neq 0$ ($\vec{k}$ is the electron-wave vector) due to the absence of inversion symmetry. Without inversion symmetry, the momentum states of $\uparrow$ and $\downarrow$ electrons are not degenerate, i.e., $E_{\vec{k}\uparrow} \neq E_{\vec{k}\downarrow}$. The resulting energy difference for electrons with the same $\vec{k}$ but different spin states plays the role of an intrinsic $\vec{k}$-dependent magnetic field or effective magnetic field [20]:

$$\vec{h}\left(\vec{k}\right) = \alpha\hbar^2\left(2em^*E_g\right)^{-1/2}\left[k_x\left(k_y^2 - k_z^2\right)\hat{x} + \mathrm{CP}\right], \qquad (1)$$

where CP stands for cyclic permutations, $\hbar = h/2\pi$ the reduced Planck constant and $\alpha$ a dimensionless, material-specific parameter, which gives the magnitude of the spin–orbit splitting and is approximately given by $\alpha \simeq 4\eta(m^*/m_{cv})/\sqrt{3-\eta}$ (where $\eta = \Delta/\left(E_g + \Delta\right)$, $m^*$ the electron's effective mass, and $m_{cv}$ a constant close in magnitude to free electron mass $m_0$), induced by the presence of the Dresselhaus (due to the bulk-inversion asymmetry) spin–orbit interaction in a zinc-blende structure, acting on the spin with its magnitude and orientation depending on $\vec{k}$. This results in spin precession (spin relaxation) with intrinsic Larmor frequency $\Omega_s\left(\vec{k}\right)$ during the time between collisions, according to the relation $d\vec{S}/dt = \Omega_s\left(\vec{k}\right) \times \vec{S}$, where $\Omega_s\left(\vec{k}\right) = (e/m^*)\vec{h}\left(\vec{k}\right)$ and $\vec{S}$ is the electron-spin polarization vector. The corresponding Hamiltonian term (DP Hamiltonian due to spin–orbital splitting of the conduction band) describing the precession of electrons in the conduction band is [20] $H_{SO}\left(\vec{k}\right) = (\hbar/2)\vec{\sigma}\cdot\Omega_s\left(\vec{k}\right)$, where $\vec{\sigma}$ is the vector of Pauli spin matrices. In a quantum well (QW), for example, the DP term is composed of the Dresselhaus term [21] and the Rashba term [22]. The Rashba term appears if the self-consistent potential within a QW is asymmetric along the growth direction and is therefore referred to as structural-inversion asymmetry contribution.

The increased electron momentum at higher electric fields brings about a stronger $\vec{h}\left(\vec{k}\right)$ and, consequently, the electron precession frequency $\Omega_s\left(\vec{k}\right)$ becomes higher. The effective magnetic field depends on the underlying material, on the geometry of the device, and on $\vec{k}$. Momentum-dependent spin procession described by the DP Hamiltonian, together with momentum scattering characterized by momentum-relaxation time, $\tau_p\left(E_{\vec{k}}\right)$, leads to spin relaxation. Since the magnitude and the direction of $\vec{k}$ changes in an uncontrolled way due to electron scattering with impurities and excitations or phonons, this process contributes to (DP) spin relaxation given by $1/\tau_s^{DP} = \gamma(\alpha/\hbar)^2\tau_p E_{\vec{k}}^3/E_g$, where $E_{\vec{k}} = k_B T$, $T$ the electron temperature, and $\gamma$ a dimensionless factor that ranges from 0.8 to 2.7, depending on the dominant momentum-relaxation process [20].

The DP spin relaxation in a bulk zinc-blende structure occurs due to the spin precession about $\vec{h}\left(\vec{k}\right)$induced by the presence of the Dresselhaus spin–orbit interaction. During transport in the electric field, electrons are accelerated to higher velocities at higher fields, where the electron temperature increases sharply due to the energy-independent nature of the dominant energy relaxation process via the longitudinal polar-optical phonon scattering [23]. The resulting high electron temperature leads to enhanced DP spin relaxation because there is large kinetic energy between successive collisions.

The $V_{sH}$ decreases rapidly with the electric field within the strong field limit, which is consistent with the results obtained in reference [24], as well as with the results of the theoretical investigation performed in reference [25], where it has been shown that for relatively low fields up to a 100-mV $\mu m^{-1}$, a substantial amount of spin polarization is preserved for several microns in gallium arsenide at room temperature and the DP spin relaxation rate increased rapidly for fields higher than 150 mV $\mu m^{-1}$ and became infinite for fields $\geq$250 mV $\mu m^{-1}$. For gallium arsenide, the Ellit–Yafet spin relaxation is less effective due to the

large energy gap and low scattering rate [20]. For *n*-doped materials, as holes are rapidly recombined with electrons due to the presence of a large number of electrons [26], spin relaxation due to the Bir–Aronov–Pikus mechanism is usually blocked in *n*-doped gallium arsenide [20]. The spin relaxation in *n*-type gallium arsenide is therefore dominated by the DP mechanism.

We now define a critical field $E_C$ for $V_{sH} = 0$, i.e., the strong field for which $V_{sH}$ completely loses or disappears. The doping density dependence of $E_C$ was calculated and is shown in Fig. 9. As can be seen, $E_C$ increases with increasing doping density in the moderate range. Here, we see that lowering the doping density shows other feature in which $V_{sH}$ becomes more field dependent, consistent with the earlier studies by Kikkawa and Awschalom [3], where they found that in bulk gallium arsenide, lowering the doping density and thus the electron kinetic energy uncovered a regime in which $\tau_s$ (and thus the spin polarization) became strongly magnetic field dependent. Principal role for the transport properties for the binary semiconductors particularly doped may also play local vacancies [26], which may also contribution to the observed transport properties due to occurrence of the local disturbances of the nano-sizes.

## Conclusions

Electron spins in *n*-doped gallium arsenide were detected and the effects of *n*-type doping in gallium arsenide under drift were studied. It was found that the effects in the spin-polarized electron transport increase with increasing doping density in the moderate range, indicating that the introduction of moderately *n*-type dopants increases $\tau_s$ or polarization in gallium arsenide. However, a high field completely destroyed the electron-spin polarization. The results were discussed based on the dominant spin-relaxation mechanism in *n*-doped gallium arsenide at room temperature.

## References

1. Ziese M, Thornton MJ (eds) (2001) In: Spin electronics, vol 569. Springer, Heidelberg
2. Das Sarma S (2001) Am Sci 89:516
3. Awschalom DD, Loss D, Samarth N (eds) (2002) In: Semiconductor spintronics and quantum computation. Springer, Berlin
4. Dyakonov MI, Khaetskii AV (2008) In: Dyakonov MI (ed) Spin Hall effect (spin physics in semiconductors). Springer, Berlin
5. Ramsteiner, Hao HY, Kawaharazuka A, Zhu HJ, Kästner M, Hey R, Däweritz L, Grahn HT, Ploog KH (2002) Phys Rev B 66:081304
6. Hammar PR, Bennet BR, Yang MJ, Johnson M (1999) Phys Rev Lett 84:203
7. Schmidt G, Ferrand D, Molenkamp LW, Filip AT, van Wees BJ (2000) Phys Rev B 62:R4790
8. Pierce DT, Meier F (1976) Phys Rev B 13:5484
9. Kato Y, Myers RC, Gossard AC, Awschalom DD (2004) Science 306:1910
10. Hirsch JE (1999) Phys Rev Lett 83:1834
11. Miah MI (2006) Mater Lett 60:2863
12. Smit J (1951) Physica 17:612
13. D'yakonov MI, Perel VI (1971) Sov Phys JETP 33:1053
14. Miah MI (2009) J Phys D Appl Phys 42:045503
15. Northrup JE, Zhang SB (1993) Phys Rev B 47:6791
16. Chazalviel J-N (1975) Phys Rev B 11:3918
17. Engel H-A, Halperin BI, Rashba EI (2005) Phys Rev Lett 95:166605
18. Tse W-K, Das Sarma S (2006) Phys Rev Lett 96:056601
19. Sanada H, Arata I, Ohno Y, Ohtani K, Chen Z, Kayanuma K, Oka Y, Matsukura F, Ohno H (2002) In: The second international conference on physics and application of spin related phenomena in semiconductors, Würzburg, Germany
20. Pikus GE, Titkov AN (1984) In: Meier F, Zakharchenya BP (eds) Optical orientation, modern problems in condensed matter science, vol 8. North-Holland, Amsterdam
21. Dresselhaus G (1955) Phys Rev 100:580
22. Bychkov YA, Rashba EI (1984) J Phys C Solid State Phys 17:6039
23. Adachi S (1994) GaAs and related materials: bulk semiconducting and superlattice properties. World Scientific, Singapore
24. Britton RS, Grevatt T, Malinowski A, Harley RT, Perozzo P, Cameron AR, Miller A (1998) Appl Phys Lett 73:2140
25. Miah MI (2008) Phys Lett A 372:6981
26. Kityk IV (2003) Semicond Sci Technol 18:1001